The dynamics of body category and emotion processing in high-level visual, prefrontal and parietal cortex.

Giuseppe Marrazzo,[1] **Maarten J. Vaessen**,[1] **Beatrice de Gelder** [1,2]

[1]Department of Cognitive Neuroscience, Faculty of Psychology and Neuroscience, Maastricht University, Limburg 6200 MD, Maastricht, The Netherlands, and [2]Department of Computer Science, University College London, London WC1E 6BT, UK

Correspondence addressed to Beatrice de Gelder, Brain and Emotion Laboratory, Department of Cognitive Neuroscience, Faculty of Psychology and Neuroscience, Maastricht University, Oxfordlaan 55, 6229 EV Maastricht, The Netherlands. E-mail: b.degelder@maastrichtuniversity.nl

| Abstract

Recent studies provided an increasingly detailed understanding of how visual objects like faces or bodies are categorized. What is less clear is whether a category attribute like the emotional expression influences category representation as is limited to extra-category selective areas and whether the coding of the expression in category and extra category areas is influenced by the task. Using functional magnetic resonance imaging (fMRI) and multivariate methods, we measured BOLD responses while participants viewed whole body expressions and performed an explicit (emotion) and implicit (shape) recognition task. Our results show that the type of task can be decoded in EBA, VLPFC and IPL with higher activity for the explicit task condition in the first two areas and no evidence of emotion specificity processes in any of them. During explicit recognition of the body expression, category representation was strengthened while action related information was be suppressed. These results provide evidence that body representations in high level visual cortex and frontoparietal cortex are task sensitive and that body selective areas differentially contribute to expression representation based on their different anatomical connectivity.

Keywords: bodies, categorization, emotion, fMRI, representational similarity analysis, dorsal-ventral stream

| Introduction

The brain encodes stimulus information in high-dimensional representational spaces based on the joint activity of neural populations (Averbeck et al. 2006; Kriegeskorte et al. 2008; Haxby et al. 2014). There is increasing evidence that this encoding process is dynamic, relatively task sensitive and that it may be at the service of different and complex behavioral goals (Hebart et al. 2018). Understanding how the brain represents the object category and its attributes is particularly relevant for body emotion expressions as the behavioral impact of body perception may vary substantially with the expression the body displays and with the task. An open question is to what extent selective attention to body images and to specific body attributes, like identity or emotional expression, influences category selectivity in body areas in ventrotemporal cortex, extrastriate body area (EBA) and the more anterior fusiform body area (FBA) (Peelen and Downing 2017; de Gelder and Poyo Solanas 2020; Ross and Atkinson 2020). Here we address two interrelated questions. First, how is the emotional expression represented in the two body selective areas EBA and FBA and in relation to the presumed specialization of these areas for body parts vs. whole bodies. Second, is body and expression representation in EBA and FBA influenced by whether or not the task requires explicit emotion recognition or are task effects limited to frontoparietal areas?

First, studies of body expression perception report an impact of emotional expression on activity in EBA and FBA (Peelen and Downing 2007; Pichon et al. 2009; 2012). Different from EBA, FBA has been suggested to have a bigger involvement in identity and emotion processing through its connections to other areas, like the amygdalae (Orgs et al. 2015). EBA and FBA may also have different roles for different emotions. For example, Peelen and colleagues found that fear significantly modulated EBA but not FBA while no difference was found in activity patterns for other expressions (Peelen et al. 2007). Traditionally such emotion specific differences have been related to differences in attention, arousal etc. More recently, these differences have also been related to different connectivity patterns. For example, it has been shown that the strength of emotion modulation in FBA is related, on a voxel-by-voxel basis, to the degree of body selectivity and is positively correlated with amygdala activation (Peelen et al. 2007). Most interestingly, the fact that EBA seems more sensitive to fearful body expressions than FBA makes more sense from

a survival point of view, since EBA has been suggested to be the interface between perceptual and motor processes (Orgs et al. 2015).

Second, it is poorly understood whether expression sensitivity of the body areas itself varies with the task, ie. whether the specific task changes how a body area represents the emotion of the body stimulus. It has been argued that the task impacts processing in prefrontal and parietal areas but not necessarily in ventral temporal category selective areas (Tsotsos 2011; Bracci et al. 2017; Bugatus et al. 2017; Xu and Vaziri-Pashkam 2019). More specifically, the task may require explicit recognition of a body attribute like the emotional expressions as opposed to incidental or implicit perception where no recognition of the expression is asked for. A classic example of implicit processing task is a gender recognition used for measuring implicit processing of facial expressions (eg. (Vuilleumier et al. 2005) or a color monitoring task used or implicit perception of body expressions (Pichon et al. 2012). For instance, we observed increased activity in FBA and EBA when participants performed an emotion versus a color-naming tasks with whole body videos (Pichon et al. 2012; Sinke et al. 2012). Implicit processing is also related to exogenous attention or stimulus driven attention, a well know source of representational dynamics (Carretie 2014). Affective stimulus attributes modulates the role of attention as shown for example with findings that bodies with fear expressions have different effects on saccades than neutral bodies (Bannerman et al. 2009) and in hemispatial neglect patients, contralesional presentation of fear body expressions reduces neglect (Tamietto et al. 2015). In an effort to disentangle the effects of attention and task, (Bugatus et al. 2017) showed that attention has an influence on category representation in high level visual cortex and in prefrontal cortex, while task did influence activity in prefrontal cortex but not in high level visual cortex. As concerns stimulus awareness, activity in ventral body category representation areas is significantly reduced for unaware stimuli but stays the same in dorsal action representation areas (Zhan et al. 2018).

The goal of this study was to investigate whether the type of task influences the representation of bodies and body expressions inside and outside body selective category areas during measurement of brain activity with fMRI. We used decoding analysis to discover how body areas are involved in explicit as opposed to implicit expression processing. If ventrotemporal body object categories areas (EBA, FBA) are relatively insensitive to task dynamics then they should not be among the

areas where task difference is observed. Alternatively, body category representation areas may be directly involved in expression recognition or indirectly through functional connectivity with other important areas in expression processing like the amygdalae (Vuilleumier et al. 2004; de Gelder et al. 2012), prefrontal areas (VLPFC) and action representation areas in parietal cortex, specifically intraparietal sulcus(IPS) and inferior parietal lobule (IPL).

Two different tasks were designed to be formally similar (similar difficulty, similar response alternatives) for use with the same stimulus materials consisting of body expressions with two different emotions and two different skin colors. One task, emotion categorization, required explicit recognition of the body expression and a forced choice between two alternatives. The other shape task required explicit recognition of a shape overlaid on the body image and a forced choice between two shape alternatives. We used multivariate decoding and RSA in order to decode stimulus and task related information in locally defined patterns of brain activity (Kriegeskorte et al. 2008; Mitchell et al. 2008; Oosterhof et al. 2010; Connolly et al. 2012; Huth et al. 2012; Sha et al. 2015; Connolly et al. 2016; Nastase et al. 2017). Our results show that the difference between the two tasks can be decoded in EBA, VLPFC and IPL and that task sensitivity is seen both in category selective areas in the higher visual cortex and in the VLPFC.

| Materials and Methods

The present study uses brain and behavioral data previously collected and described in (Watson and de Gelder 2017) but now analyzed from a different perspective and with fully different methods.

| Participants

Data of twenty Caucasian participants were used for the current study (8 males, mean age ± standard deviation=22 ± 3.51 years). Participants were naive to the task and the stimuli and received a monetary reward for their participation. Written informed consent was provided before starting the protocol. The scanning session took place at the neuroimaging facility Scannexus at

Maastricht University. All procedures conformed with the Declaration of Helsinki and the study was approved by the Ethics Committee of Maastricht University.

| **Stimuli**

Stimuli consist of still images of angry and happy body postures of black African and white Caucasian ethnicity. The set of black body expressions was obtained by instructing black African participants, all residents of Cape Town, South Africa, to imagine a range of daily events and show how they would react to them nonverbally. The set of white affective body stimuli (five males each expressing anger and happiness) were selected from a set previously validated (Stienen et al. 2011; Van den Stock et al. 2011). Both sets were pre-processed with the same software and underwent the same post-selection procedure. Photographs were captured using a Nikon V1 35mm camera equipped with a Nikon 30-100mm lens on a tripod, and under studio lighting. The photos showed the entire body, including the hands and feet. Ten white European participants were then asked to categorize the emotion expressed (neutrality, anger, happiness, fear, sadness, disgust) in a given picture. All emotions were recognized above 70%. Based on these results five male identities were chosen, with photos of each identity expressing both anger and happiness. Ten upright white and black (20 in total) affective body images were selected for the final stimulus set. Pictures were edited using Adobe Photoshop CC 14 software (Adobe System Incorporated) in order to mask the faces using an averaged skin color; thus, there was no affective information in the face. The stimulus set was composed of 20 affective bodies (2 races (Black, White) x 2 emotions (Angry, Happy) x 5 identities).

| **fMRI Acquisition and Experimental Procedure**

Participants were scanned using a Siemens 3T Prisma scanner. Padding and earplugs were used to reduce head movements and scanner noise. Stimuli were projected to the center of a semi-translucent screen at the back of the scanner bore that participants could see using a mirror mounted on the head coil. The experiment comprised two categorization tasks that followed a mixed block/event related design of four separate runs. Each run consisted of a presentation of emotion (A) and shape (B) blocks (AB – BA – BA – AB) and in each block stimuli were presented in a slow event related manner. The two different tasks were designed to provide information on explicit and implicit emotion perception. For the emotion block, participants were instructed to

respond on whether the emotion expressed was anger or happiness. In the shape block, participants judged whether the stimulus contained a circle or a square which was superimposed on the body. The task was indicated on the screen for 2 s before each block began. The trials in each block were separated by a fixation cross on a gray background that appeared for 10 or 12 s (in a pseudo-random order). Following the fixation cross, a body image was presented for 500 ms followed by a response screen lasting 1500 ms, showing the two response options on the left and right of the fixation cross and corresponding to the index and to the middle finger respectively. The side of the response options were randomized per trial to avoid motor preparation. Each stimulus was presented twice in each run, once during the emotion task and once during the shape task. Thus, each run consisted of 40 trials (+ 2 task indicators), see Fig. 1.

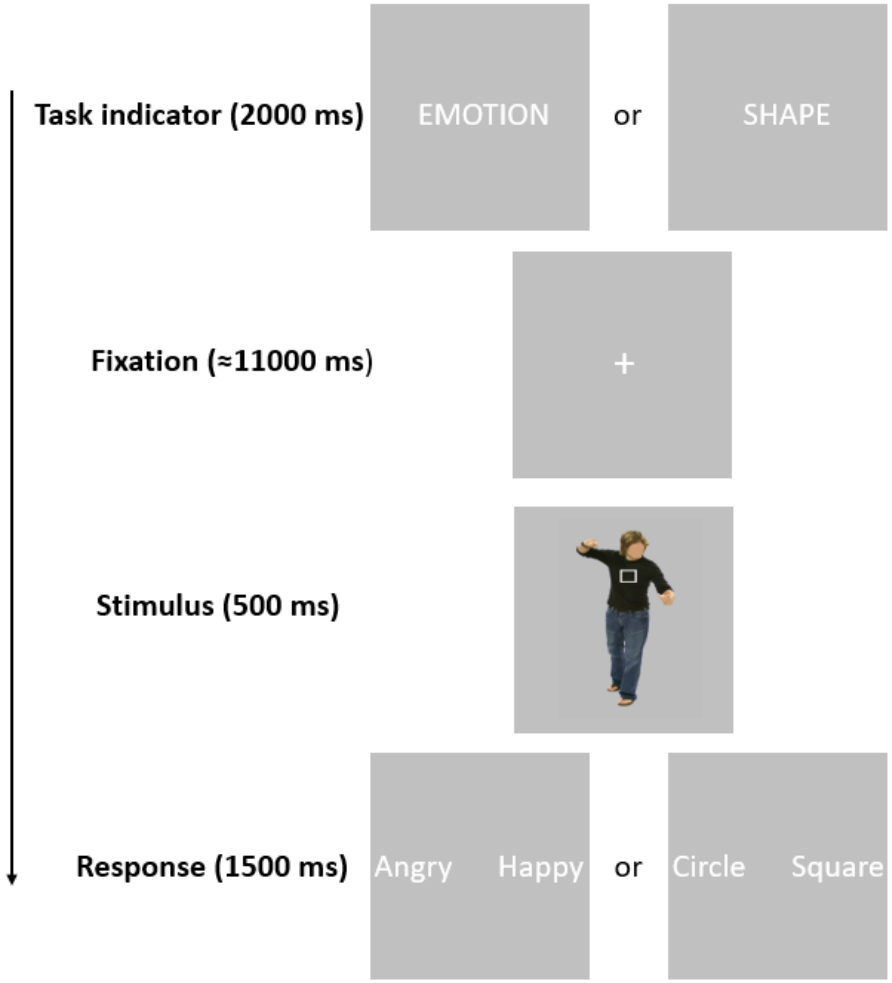

Figure 1. Examples of both explicit and implicit trials. During the experiment a task indicator appeared (2000 ms) showing which task (explicit emotional evaluation or implicit emotional evaluation)

the participants were going to perform. The task indicator was followed by a fixation period, the stimulus (white happy/angry, or black happy/angry) and a response window. Participants responded via two buttons pressed by the index finger (word on the left) and the middle finger (word on the right), with randomization of the response options in order to avoid motor preparation (*Watson and de Gelder 2017*)

| MRI acquisition and Data Preprocessing

A T2*-weighted gradient echo EPI sequence was used to acquire the functional data covering the whole brain with 2 x 2 x 2 mm^3 resolution (64 slices without gaps, TR = 2000 ms, TE= 30 ms, flip angle= 77 º, multiband acceleration factor = 2, FOV = 160 x 160 mm, matrix size = 100 x 100). Furthermore, a T1-weighted MPRAGE sequence was used for each participant (1 x 1 x 1 mm^3, TR=2300 ms, TE= 2.98 ms). Preprocessing was performed using BrainVoyager software (BrainVoyager QX) (Brain Innovation B.V., Maastricht, the Netherlands). For each run a slice scan time correction using sinc interpolation was performed, data from each run was motion-corrected by realigning to the first volume of the first run using sinc interpolation. A two-cycle temporal high-pass filtering was applied in order to remove low frequency linear and quadratic trends. Notice that no spatial smoothing was performed at this stage. The anatomical data, after the skull removal and inhomogeneity correction, were spatially warped to MNI space (MNI-ICBM 152), and the functional data were then co-registered to the anatomical data in the new space using the boundary based registration algorithm (Greve and Fischl 2009).

| Univariate Analysis

Using BrainVoyager (v21.2) (BV) we first defined a subject-specific univariate general linear model (GLM) where each condition (emotion black angry (E_BA), emotion black happy (E_BH), emotion white angry (E_WA), emotion white happy (E_WH), shape black angry (S_BA), shape black happy (S_BH), shape white angry (S_WA), shape white happy (S_WH)) was included as a square wave of the same duration of the trial, convolved with the canonical hemodynamic response function. The 3D motion parameter estimates were included as regressors of no interest in the design matrix. For the group statistical analysis, we first performed spatial smoothing with a Gaussian Kernel (3 mm) of all the functional images and then, in order to assess the variability of observed effects across subjects, we combined the individual GLM's in a random effects (RFX) GLM analysis, as is the custom in the BV pipeline. For 7 participants, only three of the five original

trials for each condition were included as predictors due to an initial error in stimulus presentation, resulting in a reduced set of 96 trials out of 160 (2 emotions x 2 skin color x 2 tasks x 5 repetitions x 4 runs). To test for effects and interactions between the factors an RFX three-way repeated measures ANOVA was performed in BV on the combined individual GLM's.

| **Multivariate Analysis**

All multivariate analyses were conducted with in-house MATLAB scripts (vR2018a, The MathWorks Inc., Natick, MA, USA). First, the BOLD time course of each voxel was divided in single trials, whose temporal window (epoch) were defined between 1TR prior and 4TR after the stimulus onset, resulting in 42 trials per run (168 in total). Within each run, 2 trials represented the task indicator and therefore they were not included in the analysis. Each trial was normalized with respect to the baseline 2000 ms, before the first stimulus onset (the first TR in the trial segment). We linearly fited the percent BOLD signal change of each voxel and each trial separately with a design matrix consisting of a constant term (intercept) and an optimized hemodynamic response function (HRF). The optimized HRF was designed to take into account potential differences in the BOLD responses (temporal delay) for a certain voxel. The optimal delay was calculated for each voxel by convolving a canonical HRF with a box-car predictor whose value was one when the stimulus was presented. The time-to-peak parameter was varied between 4.0 s and 6.0 s in steps of 0.5 s. The five resulting HRFs were fit to the percent BOLD signal change of all trials averaged and the time-to-peak giving the best fit was chosen as the optimal HRF delay of that voxel. For each trial and each voxel, we then used the resulting β-values as a feature in the classifier (Gardumi et al. 2016).

Searchlight analysis

In order to perform whole brain decoding (Kriegeskorte et al. 2006) we implemented the method proposed by (Ontivero-Ortega et al. 2017), in which the brain is divided into spheres of searchlights and a fast Gaussian Naïve Bayes (GNB) classifier is fitted in each of them. Each searchlight has a radius of 5 voxels and is defined by a central voxel and a set of voxels in its neighborhood. The classification accuracy of the searchlight region was then assigned to the central voxel. In order to avoid overfitting, for each subject we split the data following the leave-one-run-out paradigm (4 – fold cross-validation) and computed the prediction accuracy by testing

the trained classifier on left-out test data. The GNB classifier was trained to predict tasks (Emotion vs Shape), emotion (Angry bodies vs Happy bodies) or skin color (Black bodies vs White bodies). Here the responses to individual stimuli were averaged for the 8 main conditions of the experiment. The emotion and skin color effects decoding were determined both across the tasks (160 trials available for training and testing the classifier) and within the tasks (80 trials for the explicit task, 80 trials for the implicit task), for 7 participants (see Univariate analysis) only 96 trials out 160 were available for the analysis. Moreover, in order to determine interstimulus differences in the multivoxel patterns (MVPs), the GNB was trained to classify the 20 unique affective bodies (5 identities x 2 skin color x 2 emotions).

Whole brain RSA of intra- versus inter-similarities analysis

In addition to decoding with a classifier, another method to detect condition effects in MVP's is to statistically test for differences between intra- versus inter-condition MPV similarities (Peelen et al. 2010). As in the GNB analysis, for each subject and for each 5 voxel radius searchlight spanning the whole brain, we built neural RDM's by computing the dissimilarity (1 - Pearson's correlation) between the multivoxel patterns of each of the 160 trials. Next, we extracted from these RDMs the intra-condition or inter-condition elements and compared these with a two sample t-test. This test was performed for the conditions of task, emotion and skin color separately. Furthermore, we assessed task specific differences between intra- versus inter-condition MPV similarities by extracting neural RDMs for emotion and skin condition within the explicit and implicit task separately. This was performed by testing the task specific neural RDMs (80 trials per task). As mentioned in the univariate analysis, for 7 participants 2 trials for each condition were to be discarded, resulting in 96 trials (48 per each task). On a group level, for each voxel, single-subject results were tested against zero, resulting in a group two-tailed t-test.

| Group Analysis

For the group-level analysis spatial smoothing (Gaussian kernel of 3mm FWHM) was applied to the resulting maps of each individual. For the decoding analysis with the GNB classifiers the maps contained the classification accuracies minus chance level and for the inter- versus intra-condition MVP similarity analysis the maps represented the t-values from the t-test. Next, for all analyses, a statistical map was obtained by performing a two tailed t-test against zero over subjects. The

statistical threshold for the overall activation pattern was p = .05 corrected for multiple comparison using the false discovery rate (FDR).

| **Region of Interest Analysis**

We selected regions of interest (ROIs) by setting a statistical threshold of p(FDR) = .01 on the map resulting from the GNB decoding on task effect (see Results). This threshold was chosen in order to obtain spatially separated sub-clusters, as the clusters at p(FDR) = .05 consisted of only a few clusters spanning many anatomical regions (see Results). Additionally, a Cluster-Level correction was performed to eliminate small clusters using the Cluster-Level Statistical Threshold Estimator plugin (FWHM = 1 voxel, 3000 iterations) (Forman et al. 1995; Goebel et al. 2006). The multi voxel patterns were then extracted from the ROI and an RSA analysis was performed for each ROI. The Representational Dissimilarity Matrices (RDMs) were built by computing a metric of distance (1 - Pearson's correlation coefficient) between the multivoxel patterns from the 8 conditions of the main experiment. We obtained group average RDM's by first computing the RDMs at the individual level and then averaging over subjects. Additionally, for each ROI, to assess the overall activation level we plotted the group average beta values from the optimized HRF model for the different experimental conditions. We extracted beta values at the individual level by averaging the multi voxel patterns of each condition and then computed group level beta values by averaging across participants.

| Results

| Behavioral analysis

To test for any difference in performance between the two emotion and shape tasks we performed a paired t-test on the recognition accuracies at the group level on the original data (Watson and de Gelder 2017). This revealed no task difference on accuracy (mean accuracy emotion = 93.95%, mean accuracy shape = 93.15%, $p = .56$). A three-way repeated measure ANOVA on the response times showed a main effect of task and emotion ($F(1,1) = 34.58$, $p < .001$; $F(1,1) = 6.76$, $p = .018$). A paired sample t-test revealed that the mean response time for the emotion task was significantly greater compared to the shape task (mean emotion = 843.01 ± 111.77 ms, mean shape = 717.35 ± 85.44 ms, $t(79) = 8.63$ $p < .001$) and the mean response time for the angry was significantly higher than the happy conditions (mean angry = 796.61± 130.25 ms, mean happy = 763.75 ± 101.37 ms, $t(79) = 2.94$, $p = .004$). Furthermore, task affects the response times for the emotion conditions and for the skin conditions ($F(1,1) = 4.66$, $p = .044$; $F(1,1) = 30.33$, $p < .001$). When participants explicitly named the emotion, we found a significant difference in the response times with greater time needed to name an angry compared to a happy image (mean angry = 873.65 ± 114.80 ms, mean happy = 812.37 ± 101.01 ms, $t(39) = 3.23$, $p = .002$). This difference was not significant during the shape categorization task. For emotion categorization condition response times were longer for the black stimuli (mean black = 875.30 ± 102.18ms, mean white = 810.72 ± 112.82 ms, $t(39) = 4.25$, $p < .001$). In contrast, for the shape categorization task mean response time for white conditions were longer that for the black stimuli (mean black = 706.04 ± 84.37 ms, mean white = 728.66 ± 86.06 ms, $t(39) = -2.28$, $p = .002$).

| Analysis of condition effects in activation level

In the univariate analysis we tested the effect of the 3 main factors (task: Explicit vs Implicit; emotion: Angry vs. Happy; skin color: Black vs. White)and their interactions, and in order to determine the direction of the effect we computed a two-tailed t-test on each pairwise contrasts. We found significant higher responses for the explicit task in lateral occipito-temporal cortex (LOTC), medial superior frontal gyrus (MSFG), bilateral ventrolateral prefrontal cortex (VLPFC) and bilateral anterior insular cortex (AIC). Higher activation levels for the implicit task were found in bilateral superior temporal gyrus (STG), right middle temporal gyrus (MTG), right inferior parietal lobule (IPL), bilateral marginal sulcus (MS) and left anterior cingulate cortex (ACC) (see

Fig. 2 and Table 1). The contrast Angry vs. Happy bodies for all trials as well as for the emotion task trials only, revealed higher activation for happy bodies in the primary visual cortex (MNI: -13, -81, -9; t(19) = -8.01, p <.001). No significant differences in activation levels were found for Black vs. White bodies. The ANOVA showed that the only interaction which gave above threshold (p(FDR)<.05) clusters was the one between emotions and skin color (table S1 in supplementary material) see also (Watson and de Gelder 2017) for the details.

Table 1. Whole Brain Group level univariate results of Explicit vs. Implicit conditions. The table shows the regions where greater activity was found for the explicit conditions (t>0) and the implicit conditions (t<0). The t-map was thresholded at p(FDR) < .05 and cluster size corrected. Peak voxel coordinates (MNI) and corresponding t value of each surviving cluster are reported. The degrees of freedom for the t-test were 19 while for the ANOVA 1 and 19. All the results were significant at p < .001.

Brain Regions	**L/R**	**X**	**y**	**Z**	**t(19)**	**F(1,19)**
Superior temporal gyrus	R	65	-16	1	8.678***	75.525***
	L	-68	-8	-3	-7.021***	45.418**
Middle temporal gyrus	R	59	-11	-36	-6.173**	38.140**
Inferior parietal lobule	R	47	-47	32	-5.043*	25.471*
Lateral occipitotemporal cortex	R	53	-66	13	6.127**	37.647**
Marginal sulcus	R	6	-30	54	-5.396*	29.219*
Ventrolateral prefrontal cortex	R	45	25	18	8.684***	75.587***
	L	-45	17	25	5.734*	32.934*
Medial superior frontal gyrus		0	18	59	5.831*	34.040*

Anterior cingulate cortex		0	33	-11	-5.667*	32.173*
Anterior insular cortex	R	36	26	-3	7.615***	57.663***
	L	-34	22	-3	6.368**	40.571**

* p<.0001
** p<.00001
*** p<.000001

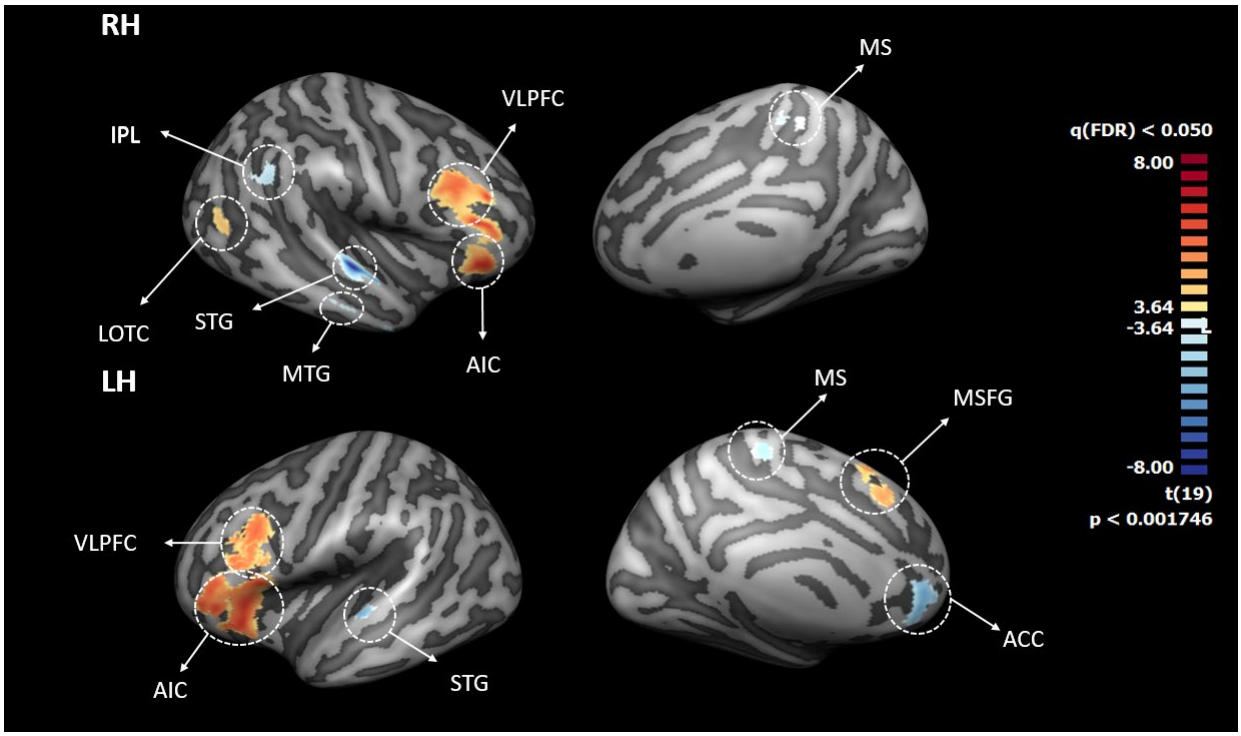

Figure 2. Whole Brain Analysis: Univariate results for Explicit vs. Implicit expression recognition task (p(FDR) < .05). The color map indicates regions where higher (red) or lower (blue) activation was found for the emotion recognition task (explicit) vs the shape recognition task (implicit). Statistical analysis was performed on the volume maps and the resulting brain regions, after thresholding, are mapped to and overlaid on the inflated group average cortical surface for visualization purposes. Abbreviations: ACC = anterior cingulate cortex, AIC = anterior insular cortex, IPL = inferior parietal lobe, LOTC = lateral-occipitotemporal cortex, MS

= marginal sulcus, MSFG = medial superior frontal gyrus, MTG = middle temporal gyrus, STG= superior temporal gyrus, VLPFC = ventrolateral prefrontal cortex.

| Multivariate decoding of task effect

The whole brain searchlight GNB analysis revealed significant above-chance classification of the explicit vs. implicit task at the group level in bilateral lateral occipito-temporal cortex (LOTC), bilateral posterior inferior temporal gyrus (PITG), posterior middle temporal gyrus (PMTG), right inferior parietal lobule (IPL), bilateral ventrolateral prefrontal cortex (VLPFC), precuneus (PCUN), posterior cingulate cortex (PCC), fusiform gyrus (FG), medial superior frontal gyrus (MSFG) and cerebellum (CB) (See Fig. 3 and Table 2 for details). Moreover, these regions overlapped substantially with the univariate GLM results as shown in Fig. 5a. Importantly, the extent and statistical significance of the multivariate GNB results where much larger than for the GLM analysis, possibly indicating that the task effect was not only expressed through the level of activation but also in different multi-voxel patterns (regardless of level of activation). We also performed an analysis of the Angry vs. Happy bodies decoding (trials of both tasks combined) and found above chance classification accuracies in the right FG (MNI: 29, -49, -20; $t(19) = 5.80$, $p < .001$) , and cerebellum (MNI: 29, -43, -34; $t(19) = 4.90$, $p < .001$). When considering the tasks separately, we did not find any regions where emotion could be decoded. When decoding Angry vs. Happy bodies (for each task separately) and Black vs. White bodies (trials of both tasks combined, and for each task separately) the classification did not yield any above chance results at the group level.

Table 2. Whole Brain Group level statistics of the classification accuracies of Explicit vs. Implicit conditions. Results produced by the searchlight GNB tested against chance level at p(FDR) < .05 and cluster size corrected (min. cluster size threshold = 176). The values of the peak voxel of each surviving cluster is reported. The degrees of freedom were 19 and p-values were less than .001. The labels in bold represent the clusters resulting from the whole brain statistical map. Regions indicated in normal font are manually defined subregions of the main clusters displayed for completeness.

Brain Regions	L/R	x	y	z	t(19)
Parietal occipitotemporal cortex					
Extrastriate body area	R	54	-59	-5	7.207**
	L	-44	-66	1	9.531***
Inferior parietal lobule	R	53	-49	25	7.448***
	L	-53	-49	25	4.957*
Intraparietal sulcus	R	35	-73	36	8.051***
	L	-27	-77	36	6.918**
Precuneus	L	-6	-68	59	7.283**
Ventrolateral prefrontal cortex	R	48	14	26	10.375***
Dorsomedial frontal cortex	L	-12	9	53	6.229**
Cerebellum	L	-10	-84	-30	5.769*

* $p<.0001$
** $p<.00001$
*** $p<.000001$

1

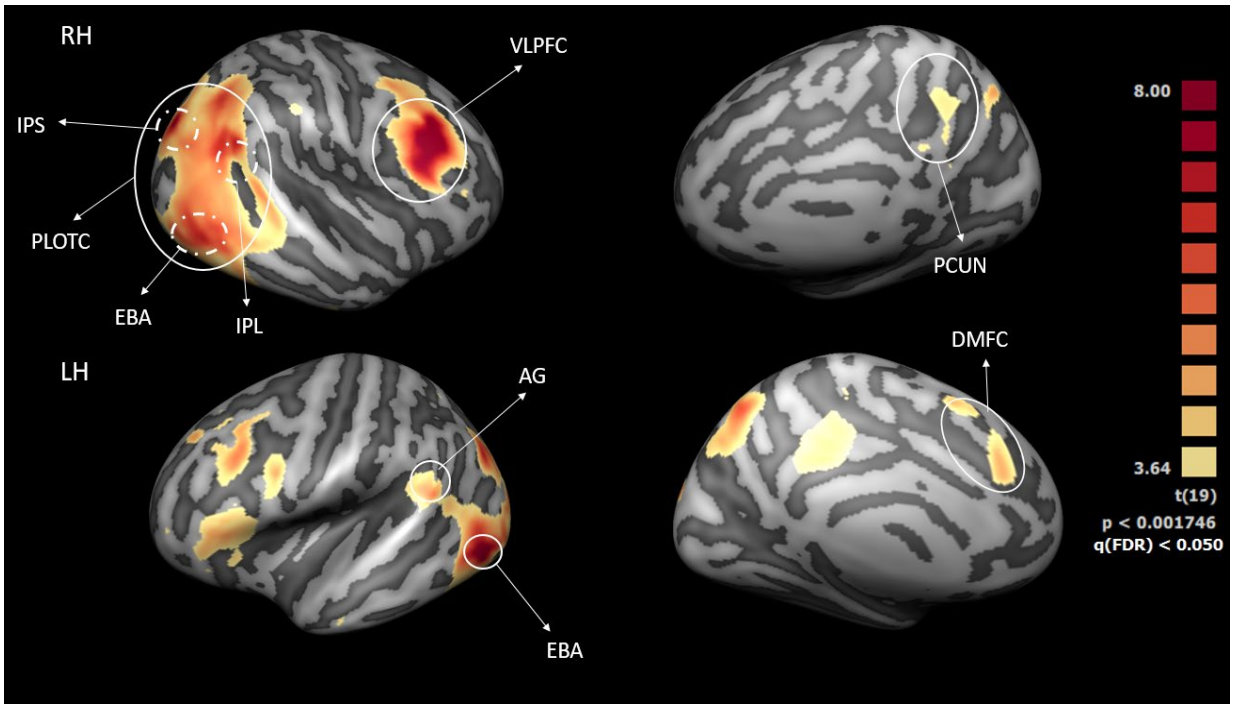

Figure 3. Whole Brain MVPA Analysis: results of the GNB classifier for Explicit vs. Implicit task. Above chance classification accuracies produced by the searchlight GNB, p(FDR) < .05 and cluster size corrected (min. cluster size threshold = 176) are shown. The color map indicates the t-value of the test against chance level accuracy. Abbreviations: AG = angular gyrus; DMFC = dorsomedial frontal cortex; EBA = extrastriate body area; IPL = inferior parietal lobe; IPS = intraparietal sulcus; PCUN = precuneus; PLOTC = parietal occipito-temporal cortex; VLPFC = ventrolateral prefrontal cortex.

| Interstimulus decoding

The 20 bodies of the stimulus set differed in a number of ways: besides the before mentioned categories of emotion and skin color, there were also person-specific variations in the details of the body pose (e.g. anger could be expressed in a different way between stimuli). This raises the question of whether these fine-grained variations in pose are part of what is encoded in body sensitive cortex. In order to check whether these differences were also reflected in the MVPs, a GNB classifier was trained to classify the 20 affective bodies. As discussed in the univariate analysis (see Materials and Methods) for 7 participants the trial set was incomplete (12 unique stimuli out of 20), therefore they were excluded from this analysis. A group two-tailed t-test against chance level was performed and the resulting t-map showed significant above chance classification accuracy (at p(FDR) <0.05), in cerebellum (t(12) = 6.84, p < .001), bilateral inferior occipital gyrus

(IOG) (right t(12) = 5.84, p < .001, left t(12) = 7.12, p < .001), fusiform gyrus (FG) (t(12) = 5.62, p < .001), primary visual cortex (V1) (t(12) = 4.61, p < .0018) (see Fig. 4).

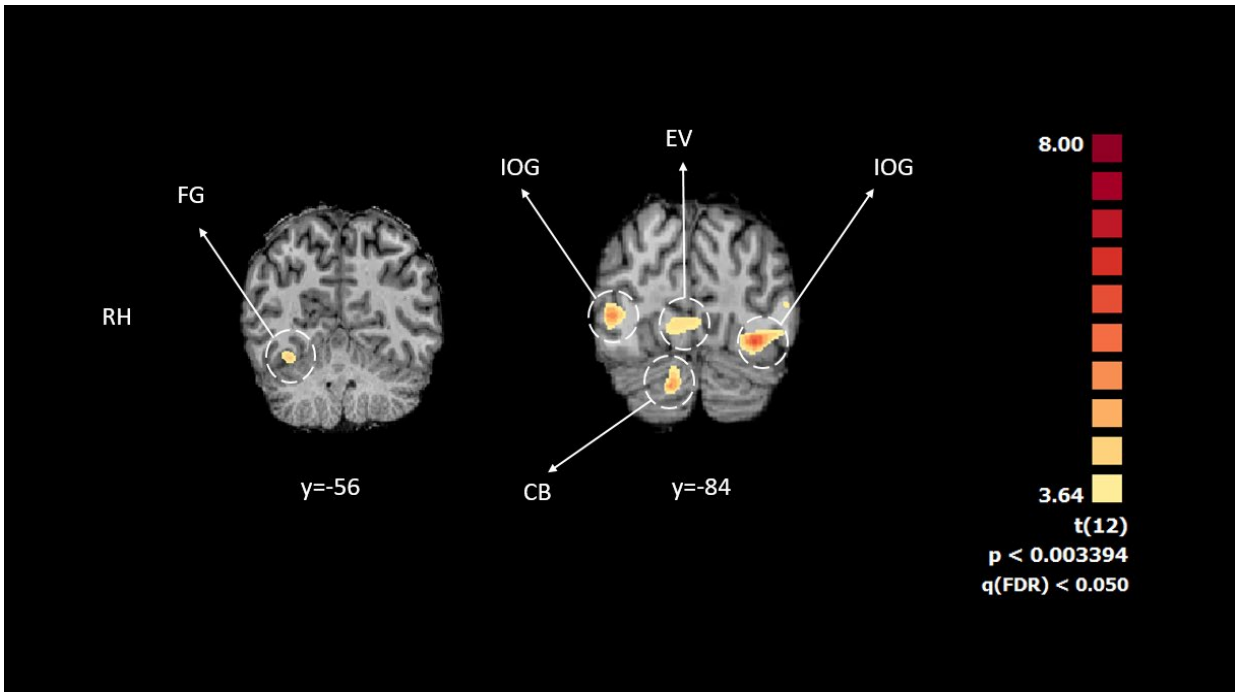

Figure 4. GNB decoding results for all 20 expressive body stimuli. Above chances classification accuracies produced by the searchlight GNB, p(FDR) < .05 for the interstimulus differences are shown. The color map indicates the t-value of the test against chance level accuracy. Abbreviations: CB =cerebellum; EV =early visual cortex; FG =fusiform gyrus; IOG =inferior occipital gyrus.

| RSA of condition effects of multivoxel similarities

In order to determine condition specific (task, emotion, skin) differences in the neural RDMs, we computed for each subject a task specific two sample t-test of intra-condition similarities (e.g. happy-happy, black-black, explicit-explicit) against inter-condition similarities (e.g. angry-happy, black-white, explicit-implicit). When analyzing MVP similarities within the tasks (intra) and between the tasks (inter) we found higher intra-task similarities in bilateral VLPFC, right superior temporal sulcus (STS), bilateral IPS and DMPFC (see Table 3). Here also, we found substantial overlap of results with the GLM and GNB analysis, see Fig. 5b.

Table 3. Whole Brain Group level statistics of RSA's condition specific (task, emotion, skin) effects of multivoxel similarities, at p(FDR) < .05. The table shows the brain regions presenting a higher intra-condition similarity (e.g. happy-happy, black-black, explicit-explicit) (t>0) and those with a higher inter-condition similarities (e.g. angry-happy, black-white, explicit-implicit) (t<0). The t values refer to the peak voxel of each surviving cluster. The degrees of freedom were 19 and p-values were less than .001.

Brain Regions	L/R	x	y	z	t(19)
Task					
Superior temporal sulcus	R	55	-17	-15	4.658*
Intraparietal sulcus	R	31	-51	40	4.704*
	L	-22	-49	41	4.740*
Dorsomedial prefrontal cortex	L	-13	22	52	4.699*
Ventrolateral prefrontal cortex	R	48	9	29	7.253***
	L	-31	31	11	5.343***
Skin color (Explicit)					
Intraparietal sulcus	L	-26	-65	53	-4.598*
Skin color (Implicit)					
Superior temporal sulcus	L	-53	-48	9	-6.131***
Ventromedial prefrontal cortex	R	20	48	15	-4.862*
Intraparietal sulcus	R	49	-34	47	-4.982**
Dorsomedial prefrontal cortex	R	6	37	43	-5.605**
Inferior parietal lobule	R	50	-47	29	-7.374***
Precuneus	L	-8	-47	38	-5.168**

Posterior cingulate cortex	L	-8	-47	13	-6.548***
Superior frontal lobe	R	15	4	60	-6.460***
Fusiform gyrus	R	20	-41	-11	-6.835***
Cuneus	L	-8	-89	37	-5.431**
Temporal lobe	L	-37	3	-23	-6.174***
Emotion (Explicit)					
Insula	L	-33	31	-3	4.101*
Postorbital gyrus	L	-24	18	-15	4.097*
Enthorinal cortex	R	26	-7	-42	-4.904**
Hippocampus	R	19	-39	-1	-5.604***
Fusiform body area	L	-39	-78	-20	-4.748*
Emotion (Implicit)					
Parahippocampal gyrus	R	21	-15	-31	4.295*
Dorsomedial prefrontal cortex		0	44	47	-7.043***
Precuneus	L	-4	-41	49	-4.358*
Premotor cortex	R	39	-16	50	-5.764**
Inferior occipital gyrus	L	-25	-92	-9	-5.185**
Superior temporal gyrus	L	-42	-35	6	-6.252***
Supramarginal gyrus	L	-55	-45	19	-7.018*

* $p<.001$
** $p<.0001$
*** $p<.00001$

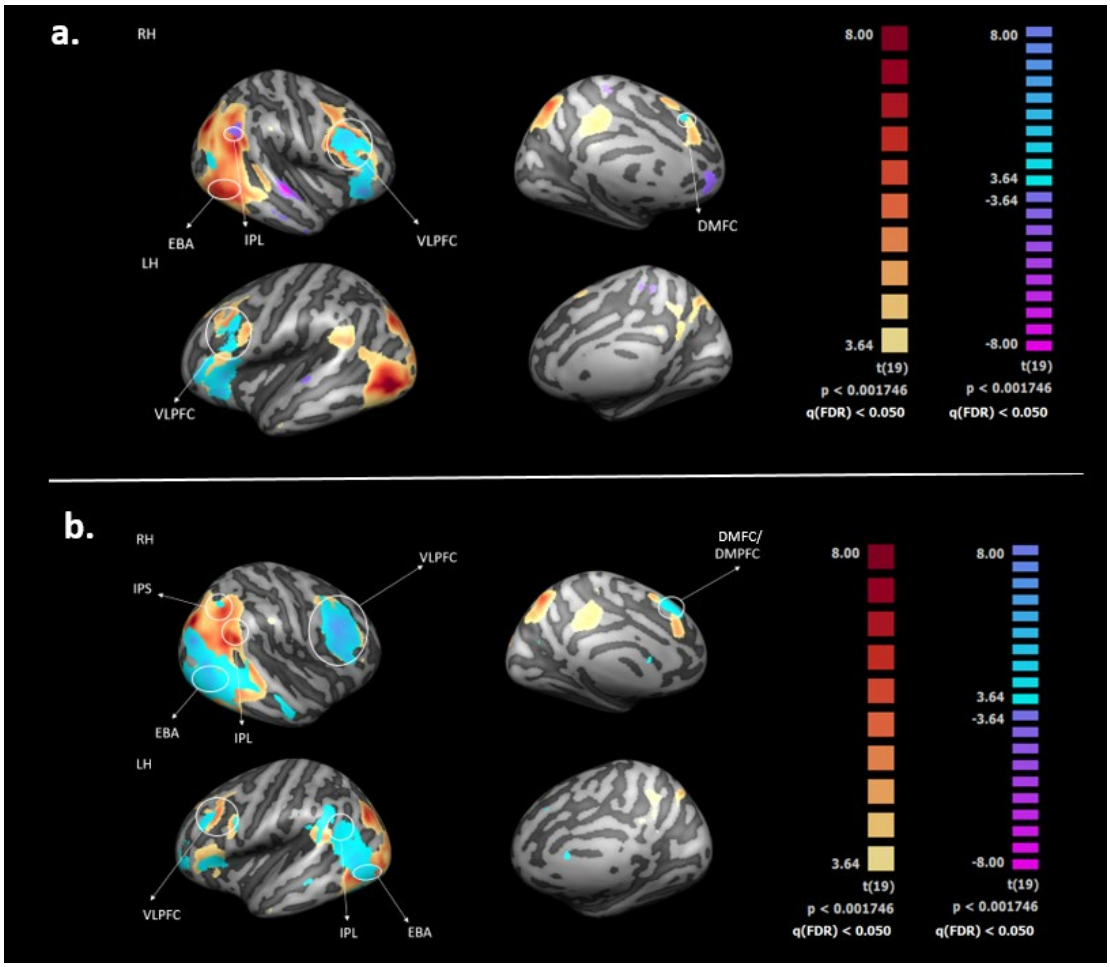

Figure 5. (a): Whole Brain MVPA and Univariate results overlap: Combined map of the results of tasks comparison (Emotions vs. Shape), mapped to and overlaid on the inflated group average cortical surface, for searchlight GNB (red-yellow) and univariate (blue-purple) results showing the extent of the overlap in RH for VLPFC, IPL and EBA. Abbreviations: DMFC = dorsomedial frontal cortex; EBA = extrastriate body area; IPL = inferior parietal lobe; VLPFC = ventrolateral prefrontal cortex.

(b): Overlap between GNB results and intra/inter condition similarities between the explicit and the implicit task. Shown in light blue-purple are the resulting areas of the inter/intra task similarities analysis at p(FDR) < .05. In order to qualitatively assess the overlap, we superimposed this map on the above chance classification accuracies produced by the searchlight GNB, p(FDR) < .05 (as in Fig. 4), shown in red-yellow. The positive values (light blue) represent regions which show a higher intra-tasks similarity.

Abbreviations: DMFC = dorsomedial frontal cortex; DMPFC = dorsomedial prefrontal cortex; EBA = extrastriate body area; IPL = inferior parietal lobe; IPS = intraparietal sulcus; PLOTC = posterior lateral occipitotemporal cortex; VLPFC = ventrolateral prefrontal cortex.

In the explicit emotion recognition task at p(FDR) = .05, higher similarities between same emotions (higher intra-similarities) are seen in left insula, left post-orbital gyrus, whereas higher similarities between different emotions (higher inter-similarities) were found in right entorhinal cortex, right hippocampus, left FBA (see Fig. 6 and Table 3).

In the implicit emotion recognition task, higher similarities were found between same emotions (higher intra-similarities) in right parahippocampal gyrus, whereas higher similarities between different emotions (higher inter-similarities) were found for dorsomedial prefrontal cortex, left precuneus, right premotor cortex, left inferior occipital gyrus, left superior temporal gyrus, left supramarginal gyrus (see Fig. 6 and Table 3).

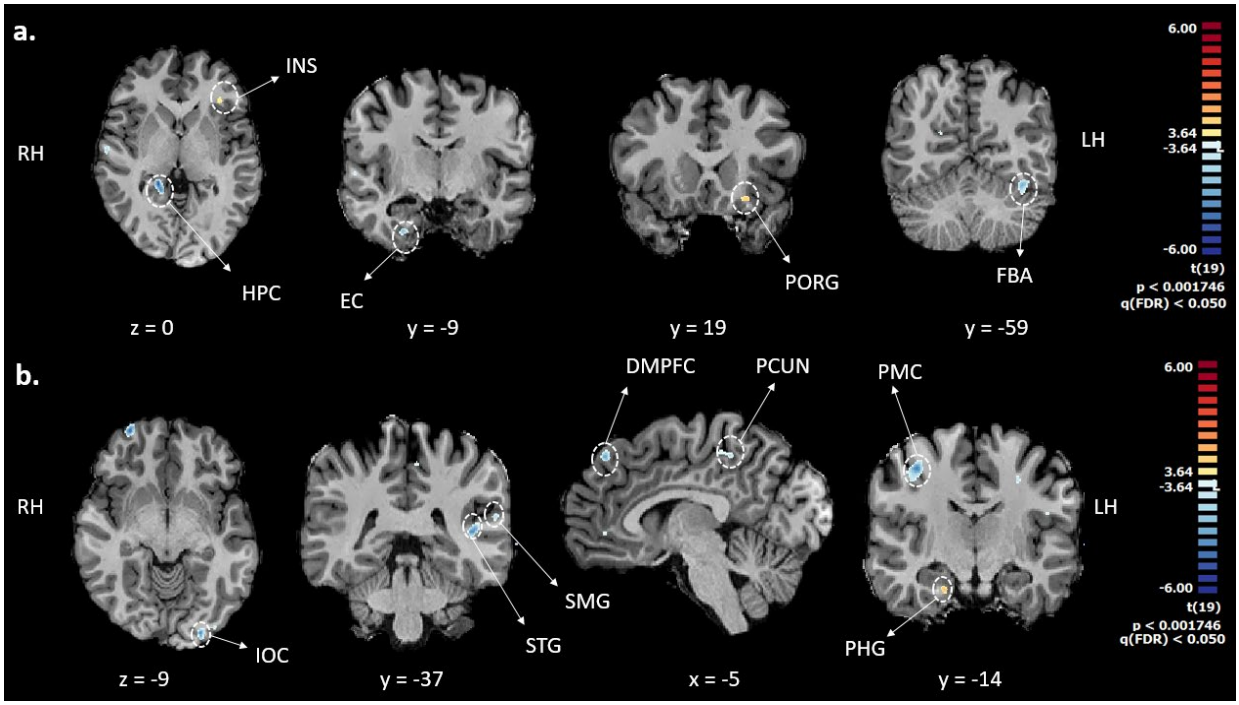

Figure 6. Inter/Intra emotion similarities analysis: Task specific results for affective body postures (angry, happy) in explicit (a) and implicit (b) emotion recognition. Group results of the two-sample t-test between intra-emotions similarities against inter-emotions similarities at p(FDR) < .05. Panel a

(explicit task) and panel b (implicit task) represent brain regions in which neural RDMs for same emotions are more similar than the neural patterns for different emotions (red) and vice versa (blue). Abbreviations: EC = entorhinal cortex; HPC = hippocampus; INS = insula; DMPFC = medial prefrontal cortex; PMC = premotor cortex; PORG = post-orbital gyrus.

Within the explicit task, higher similarities between different skin colors (higher inter-similarities) were found in left IPS. Similarly, in the implicit task higher similarities between different skin colors (higher inter-similarities) were found for DMPFC, ventromedial prefrontal cortex (VMPFC), left precuneus, right IPS, right IPL, right superior frontal lobe (SFL), left temporal lobe, left cuneus, left PCC, right FG, left PSTS (see Fig. 7 and Table 3).

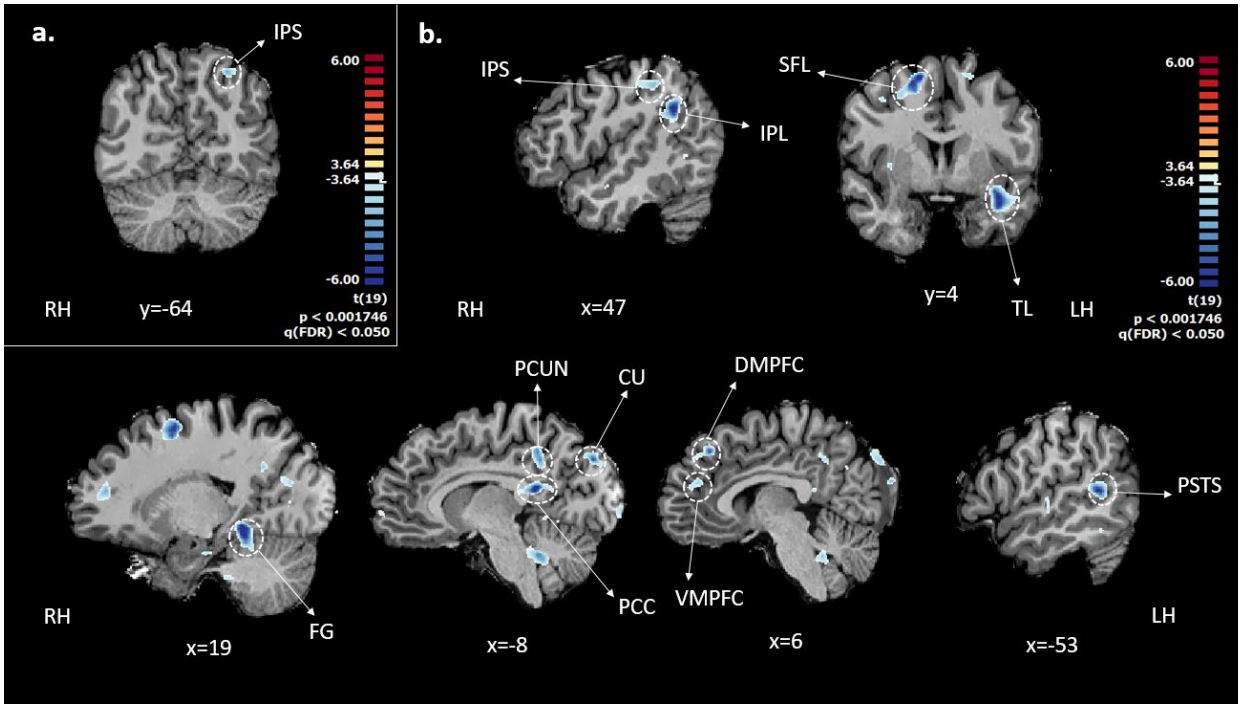

Figure 7. Inter/Intra condition similarities analysis: Task specific results for skin colors (black, white) in explicit (a) and implicit (b) emotion recognition. Group results of the two-sample t-test between intra-condition (e.g. black-black) similarities against inter-conditions similarities (e.g. black-white) at p(FDR) < .05. Panel (a) and panel (b) represent brain region in which neural RDMs for same emotions are more similar than the neural patterns for different emotions (red) and vice versa (blue) for the explicit task and implicit task respectively. Abbreviations: CU = cuneus; DMPFC = dorsomedial prefrontal cortex; FG = fusiform gyrus; IPL = inferior parietal lobule; IPS = intraparietal sulcus; VMPFC

= medial prefrontal cortex; PCC = posterior cingulate cortex; PCUN = precuneus; PSTS = posterior superior temporal gyrus; SFL = superior frontal lobe; TL = temporal lobe.

| Region of Interest Analysis

All three analyses on task effect (univariate GLM, multivariate GNB and RSA) revealed convergent results spanning a number of anatomical regions (Fig. 3), e.g. VMPFC, IPL and LOTC (including EBA). To gain more insight into the details of the responses in these regions, we defined several ROIs by setting a statistical threshold of p(FDR) = 0.01 cluster size corrected (min. cluster size threshold = 34) on the maps of the GNB analysis and extracting beta values from the resulting clusters. For the explicit vs. implicit task decoding this revealed bilateral EBA, right IPL, right VLPFC, precuneus, and bilateral IPS, see Table 4.

Table 4. Region of interest (ROIs). Group level statistics of the classification accuracies produced by the GNB of Explicit vs. Implicit conditions tested against chance level**,** at p(FDR) < .01 and cluster size corrected (min. cluster size threshold = 34). The values of the peak voxel of each surviving cluster is reported. The degrees of freedom were 19 and p-values were less than .001.

Brain Regions	**L/R**	**x**	**y**	**z**	**t(19)**
Extrastriate body area	R	54	-59	-5	7.207***
	L	-44	-66	1	9.531***
Inferior parietal lobule	R	53	-49	25	7.448***
Intraparietal sulcus	R	35	-73	36	8.051***
	L	-27	-77	36	6.918**
Precuneus	L	-6	-68	59	7.283***
Ventrolateral prefrontal cortex	R	48	14	26	10.375***

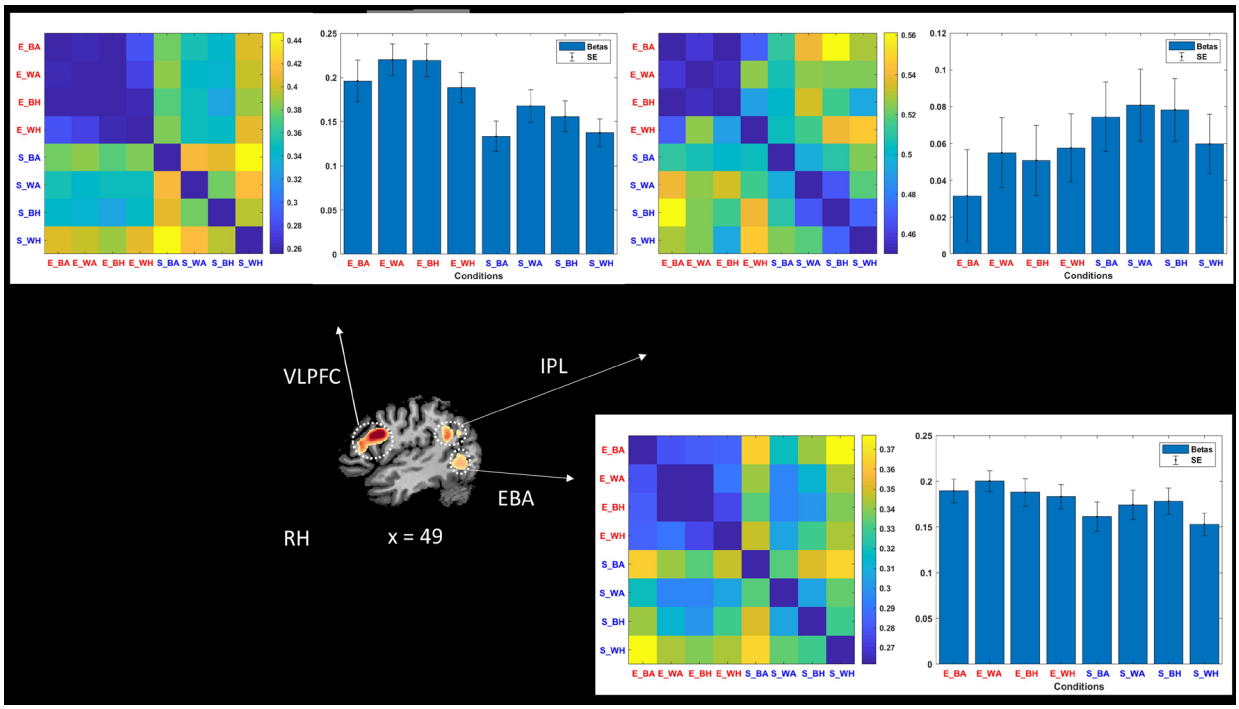

Figure 8. Details of the responses from the ROIs identified by the task based decoding, RDM and beta plots at the category level of each ROIs are shown. The different ROIs are the result of the classification accuracies tested against zero produced by the GNB thresholded at p(FDR) = 0.01 cluster size corrected (min. cluster size threshold = 34). On the left side of the panels the RDMs computed with 1-Pearson's correlations distance between the different conditions are shown. The bar charts on the right side of the panel show the mean plus standard error of the group averaged ROI beta values. The RDM for VLPFC and (right) EBA show a pattern of similarities within the explicit condition however, the same pattern is absent in the implicit condition. The condition's color labels refer to the explicit recognition task (red) and implicit recognition task (blue). Abbreviations: EBA = extrastriate body area; IPL = inferior parietal lobe; VLPFC = ventrolateral prefrontal cortex.

As shown in Fig. 8, the neural RDMs of the EBA and VLPFC ROIs show a similar structure, in particular in the explicit task conditions (upper left half of the RDM), whereas this effect is absent in the implicit conditions (bottom right half of the RDM). In order to formally assess the differences between the dissimilarities of the implicit compared to the explicit task, a two tail t-test was performed. This revealed significant differences in right EBA ($t(19) = -6.36$, $p < .001$), left EBA ($t(19) = -3.93$, $p < .003$), right VLPFC ($t(19) = -14.07$, $p < .001$) and left IPS ($t(19) = -4.82$, $p < .001$). The mean ROIs voxel activation levels were significantly higher for the explicit conditions compared to the implicit ones for VLPFC ($t(19) =4.42$, $p < .001$), and right EBA ($t(19)=$

2.36, p=0.019) which was also reflected in the univariate results (see Fig. 2). While the MVPs of the other regions (see supplementary material, Figs S1 and S2) produce RDMs which present effects (similarities or dissimilarities) within conditions or activation levels, they do not show the clear pattern found for EBA and VLPFC.

| Discussion

In the present study we measured the representational dynamics of explicit and implicit body expression perception and identified the brain areas that are critical for the distinction between the two tasks. Our results revealed three main findings. First, the difference between explicit and the implicit body expression processing can be decoded with high accuracy in EBA, VLFPC and IPL. Second, explicit recognition activity in these areas is not emotion specific. Third, condition specific effects for differences between expressions are observed in the implicit condition. In the sections below we discuss these findings and propose that taken together these findings suggest that the way in which object category, stimulus attributes and action are represented is dynamically organized by the requirements of each task and we clarify the functional role of body areas.

| *Similar task specificity across high-level visual cortex, VLFPC and IPL.*

The first major result of our study is that these are three areas where the difference between naming the expression or naming a shape on top of it and ignoring the expression can be decoded with high accuracy, and mainly expressed through highly similar responses for all conditions in the explicit task. Our results are consistent with previous studies that have reported task specific activity in higher visual cortex and VLPFC (Kriegeskorte et al. 2008; Pichon et al. 2009; Haxby et al. 2014; Bracci et al. 2017; Bugatus et al. 2017; Xu and Vaziri-Pashkam 2019). Specifically concerning explicit tasks, increased sensitivity in higher visual areas was found in some but not in other earlier studies. A previous study (Bugatus et al. 2017) found that during either a working memory, oddball or selective attention task, the task effect was limited to VLPFC and not seen in high-level visual cortex where responses were more driven by stimulus category than by the task demands. One explanation for the same task effect for EBA and VLPFC here is that VLPFC contains flexible category representations (here body specific neurons) when the task requires it (Bugatus et al. 2017). While this may explain the task sensitivity to body expression categorization in VLPFC, it does not address the finding of task sensitivity in EBA. An alternative explanation that would clarify the similar task effect in EBA and VLPFC is that the explicit task effect we see here is in fact a selective attention effect. Perception driven by selective attention to the expression might then have a region-general effect across EBA and VLPFC. This is in agreement with studies showing that selective attention alters distributed category representations across cortex, and

particularly in high-level visual cortex and VLPFC (Peelen et al. 2009; Cukur et al. 2013). Our results are consistent with this to some extent. These studies found effects of attention on category representations in high-level visual cortex when the task included visual competition. However, an argument against this explanation is that we do not find a task effect in the implicit task condition that is using identical materials and task demands. Finally, selective attention to the body expressions in the explicit task may boost body representation but presumably similar in EBA and FBA.

| ***Task dynamics, body and body representation in EBA.***

EBA and FBA are commonly viewed as ventral stream areas associated with body representation, but their respective functions are not yet clear nor is their anatomy well understood (Weiner and Grill-Spector 2012). Whole body perception is attributed more to FBA than to the EBA which is seen as more involved in body parts (Downing et al. 2001; Peelen and Downing 2007). Few studies have yet investigated the specific functional roles of FBA and EBA either in expression perception or in relation to task demands and available studies find no clear differences in their functional role for expression and task sensitivity. Our results contribute to clarifying this situation.

Considering their category sensitivity, the current view is that EBA encodes details pertaining to the shape, posture and position of the body and does not directly contribute to high level percepts of identity, emotion or action that are potential functions of FBA through its connections with other areas (Downing and Peelen 2011). However, studies on body expressions have most often reported involvement of both EBA and FBA with the activity pattern varying with the specific expression considered but without any clear understanding of the respective functions (Costantini et al. 2005; Saxe et al. 2006; Moro et al. 2008; Marsh et al. 2010; Pichon et al. 2012; de Gelder et al. 2015; Tamietto et al. 2015; Van den Stock et al. 2015).

Recent evidence offers a more detailed view on EBA and how it could contribute differentially to body and body expression perception rather than FBA which is consistent with our present findings. First, an investigation aimed at sorting out the function of EBA and adjacent MT+ reported a double dissociation, with TMS over EBA disrupting performance in the form discrimination task significantly more than TMS over pSTS, and *vice-versa* for the motion

discrimination task (Vangeneugden et al. 2014). Additionally, (Zimmermann et al. 2016) showed that early disrupting of neuronal processing in EBA during action planning, causes alterations in goal-oriented motor behavior. Second, in support of the difference found here, EBA and FBA show a very different profile of anatomical connectivity with other brain areas, notably with parietal areas (Zimmermann et al. 2018). Third, EBA is a complex area with important subdivisions (Weiner and Grill-Spector 2011). In a recent study investigating detailed features of body expressions and how they are represented in the brain, major differences in the functional role of EBA and FBA when studied at the feature coding level were found (Poyo Solanas et al. 2020). EBA and FBA also showed tuning to postural features of different expressions. However, the stimulus representation in EBA was very dissimilar to that of FBA. Similar feature representation to that seen in EBA was found in SMG, pSTS, pIPS and the inferior frontal cortex but not in FBA (Poyo Solanas et al. 2020). Such evidence marks a beginning in understanding more fine grained details of how category selective areas implement their role. When such findings targeting function descriptions at the feature level accumulate, more detailed theories about task impact can be formulated.

| *The role of IPL*

In IPL like in EBA and in VLPFC, we are able to decode the difference between the tasks, albeit less clearly and with higher beta values for the implicit condition. In the univariate results also, IPL is more active in the implicit task. IPL is a hub structure as it is involved in at least four networks (the frontoparietal, default mode, cingulo-opercular and ventral attention network (Igelström and Graziano 2017). Previous studies provided clear evidence for the role played by IPL in body and emotional perception. Emotion-specific activation within parietal cortex was found for face stimuli (Grezes et al. 2007; Kitada et al. 2010; Sarkheil et al. 2013) and for body stimuli (de Gelder et al. 2004; Kana and Travers 2012; Goldberg et al. 2014; Goldberg et al. 2015). Significant activity was elicited in IPL when contrasting bodies expressing fear and happiness (Poyo Solanas et al. 2018). We argued previously that IPL may play the role of a hub in which emotion perception is transitioned into an action response (Engelen et al. 2018). IPL receives input from the visual system (Caspers et al. 2011) and has connections to pre-motor cortex involved in action preparation (Makris et al. 2005; Hoshi and Tanji 2007; Mars et al. 2011).

But unlike VLPFC and EBA activity levels in IPL, there is a trend for beta values to be higher in the shape task. Concerning the reversal of the pattern seen in IPL compared to that of EBA and VLPFC activity, higher activity in IPL in the implicit task fits the role of IPL in action representation and its involvement in the transition to action preparation (Engelen et al. 2018). Explicit emotion recognition is a cognitive task and in the course of using verbal labels action tendencies triggered by the stimuli are suppressed, which may be reflected in lower IPL activity (Engelen et al. 2015; Igelström and Graziano 2017). In line with this, there is no difference between the emotion conditions in the explicit task while there is a suggestion of this in the implicit task (but this is not significant).

| *The role of VLPFC*

Similar to the results for EBA we found that activity in right VLPFC allows decoding the task difference, again with significantly higher beta values for the explicit task and with no difference between the expression conditions. In the whole-brain RSA, VLPFC showed higher intra-task similarity (higher similarity for same task) (see Fig. 5 and Table 3), consistent with the pattern of similarities we found in the RDMs during the ROIs analysis (see Fig. 8). Possible explanations for the role of VLPFC are its role in attention and decision making, or the possibility that VLPFC contains object category representations and finally, the fact that VLPFC plays a role in affective processes.

A familiar function of VLPFC is related to theories of PFC as predominantly involved in attention and decision processes (Duncan 2001; 2010) and it associates VLPFC activity with increased task demands (Crittenden and Duncan 2014). At a general level, this explanation does not clearly seem to fit the current results. Our two tasks were designed to be very similar in difficulty and in task demands and required a simple forced choice between two alternative responses. Under these circumstances one would not expect a task related difference in VLPFC and task independent automatic processing would proceed in both task conditions (de Gelder et al. 2012) and presumably be emotion condition specific. To understand the role of VLPFC here, a question is whether the focus on cognitive labelling in the emotion task suppressed more strongly automatic expression processing than the shape task.

A different explanation for the role of VLPFC relates to the involvement of PFC in emotion processes. Previous studies have shown that the VLPFC is involved in downregulating emotion responses by its structural and functional connectivity to the amygdala (Wager 2008). As shown by (Chick et al. 2019) when TMS is used on VLPFC, processing of emotional facial expressions is interrupted. Consistent with this explanation we find that beta values are higher in VLPFC for explicit recognition conditions. In line with that also, this increased VLPFC activity would then be expected to be stimulus condition specific (Jiang et al. 2007; McKee et al. 2014), but we find no condition specific effects. This raises the question of whether there is a pattern in the expression specific activity that could throw light on the role of VLPC

| ***Explicit vs implicit task representation of emotions.***

A first finding in the RSA is that decoding accuracies for emotion were overall low and did not differ between the emotion and the shape task. It is worth noting that the amygdalae are not among the areas we found important for task decoding. Many studies have argued that the amygdala is activated for stimuli with affective valence whether due to fear, anger of happy expressions, or overall stimulus salience and that often activity is lower under the implicit viewing conditions (di Pellegrino et al. 2005; Habel et al. 2007; de Gelder et al. 2012). Our analysis does not reveal amygdala as an area where the difference comes up in decoding accuracy when implicit and explicit tasks are compared. This is consistent with the literature showing activation in amygdala both in explicit as well as in implicit emotion evaluation, albeit somewhat lower in the latter condition (de Gelder et al. 2012). The GNB classifier used for the analysis was trained to find regions with large differences in the MVPs for the explicit task and the implicit task and it is thus not surprising that we do not find amygdala with this analysis.

In the Intra/Inter RDMs similarities analysis (Fig. 6,7) specifically looking for emotion condition effects, we did observe an overall pattern of task and emotion representation dynamics. Overall, similarities and differences between the emotion conditions do not overlap for the two tasks. For the explicit emotion recognition task, higher similarities between same emotions were seen in left insula and left post-orbital gyrus. Interestingly, these areas are found when body expressions are seen consciously but not when they are unattended or neglected (Tamietto et al. 2015; Salomon et al. 2016). For the implicit emotion recognition task, higher intra emotion similarities were found

in right parahippocampal gyrus, which may reflect that processing expressions involves memory similarly for both expressions. For the explicit task, higher similarities between different emotions representing what is common to different emotions, were found in right entorhinal cortex, right hippocampus and left FBA. Concerning the latter, this suggest that FBA is involved in expression recognition but does not contribute to specific expression coding. In contrast, in the implicit task higher similarities between different emotions were found in medial prefrontal cortex, left precuneus, left premotor cortex, right inferior occipital gyrus, right superior temporal gyrus and right supramarginal gyrus. Interestingly, the latter are all areas known from studies that used passive viewing or oddball tasks and not emotion labeling or explicit recognition (de Gelder et al. 2004; Grezes et al. 2007; Goldberg et al. 2015).

| *Limitations and future perspectives.*

The present study used two body expressions and leaves open whether the same pattern would be observed with different expressions. Besides its theoretical importance for understanding how different viewing modalities affect how emotional expressions are processes by the brain, the difference between implicit and explicit affective processes has important clinical correlates. A wealth of studies have shown that using implicit measures allows for a more nuanced and sometimes different assessment of social and communication disorders. For example, in autism as well as in schizophrenia it has been reported that implicit measures are more diagnostic than explicit ones (Van den Stock et al. 2011; Luckhardt et al. 2017; Hajdúk et al. 2019). In studies on autism spectrum and eating disorders EBA and pSTS abnormalities have been reported (Ross et al. 2019)). A better understanding of implicit processing as seen in real life routines and explicit recognition as seen in questionnaires will shed new light clinical findings and provide a rich analytical framework for investigating other social cognitive disorders.

| Conclusion

The main purpose of this study was to investigate how explicit and implicit emotion perception affected the role of body category and emotion coding areas during the processing of whole body expressions and to assess whether the activity patterns would also reflect differences between emotional expression and skin colors. Reviewing the various alternatives for the respective role of

EBA, VLPFC and IPL related to the task driven dynamics, the results suggest that EBA may be active in response to explicit body attribute recognition, and the parallel pattern in VLPFC may itself play a role either because it also codes for body category when the task demands it and/or it plays a role in emotion regulation that may be involved when the task requires verbal naming. However, we can relate the EBA and VLPFC results to the role of IPL related to action observation and preparation as discussed above. The finding of task discriminative activity in IPL suggests that the higher similarities in the explicit emotion task for VLPFC and EBA are not just independently reflecting stimulus/task settings and higher activation level in the explicit emotion task. The combination of higher activation in EBA and VLPFC and lower activation in IPL suggests connections between them with VLPFC possibly influencing EBA positively and IPL negatively (Goldman-Rakic 1996; Ongur and Price 2000; Craig 2009; Tamietto et al. 2015; Ong et al. 2019). For the task of explicit recognition of the body expression, category representation would be strengthened while action related information would be suppressed. Overall, this result indicates that the similarities found in explicit tasks do not map onto the pattern of the implicit ones and stress the importance of reckoning with the task being used to investigate the brain correlates of affective processes and reach conclusions about socio-affective impairments.

| Acknowledgements

This work was supported by the European Research Council (ERC) FP7-IDEAS-ERC (Grant agreement number 295673 Emobodies), by the Future and Emerging Technologies (FET) Proactive Programme H2020-EU.1.2.2 (Grant agreement 824160; EnTimeMent) and by the Industrial Leadership Programme H2020-EU.1.2.2 (Grant agreement 825079; MindSpaces). We are grateful to M. Zhan and M. Poyo Solanas for valuable comments and suggestions on an earlier version.

| References

Averbeck BB, Latham PE, Pouget A. 2006. Neural correlations, population coding and computation. Nat Rev Neurosci 7(5):358-66.

Bannerman RL, Milders M, de Gelder B, Sahraie A. 2009. Orienting to threat: faster localization of fearful facial expressions and body postures revealed by saccadic eye movements. Proceedings of the Royal Society B-Biological Sciences 276(1662):1635-1641.

Bracci S, Daniels N, Op de Beeck H. 2017. Task Context Overrules Object- and Category-Related Representational Content in the Human Parietal Cortex. Cerebral Cortex 27(1):310-321.

Bugatus L, Weiner KS, Grill-Spector K. 2017. Task alters category representations in prefrontal but not high-level visual cortex. Neuroimage 155:437-449.

Carretie L. 2014. Exogenous (automatic) attention to emotional stimuli: a review. Cognitive Affective & Behavioral Neuroscience 14(4):1228-1258.

Caspers S, Eickhoff SB, Rick T, von Kapri A, Kuhlen T, Huang R, Shah NJ, Zilles K. 2011. Probabilistic fibre tract analysis of cytoarchitectonically defined human inferior parietal lobule areas reveals similarities to macaques. Neuroimage 58(2):362-380.

Chick CF, Rolle C, Trivedi HM, Monuszko K, Etkin A. 2019. Transcranial magnetic stimulation demonstrates a role for the ventrolateral prefrontal cortex in emotion perception. Psychiatry Research:112515.

Connolly AC, Guntupalli JS, Gors J, Hanke M, Halchenko YO, Wu YC, Abdi H, Haxby JV. 2012. The Representation of Biological Classes in the Human Brain. Journal of Neuroscience 32(8):2608-2618.

Connolly AC, Sha L, Guntupalli JS, Oosterhof N, Halchenko YO, Nastase SA, Castello MVD, Abdi H, Jobst BC, Gobbini MI et al. . 2016. How the Human Brain Represents Perceived Dangerousness or "Predacity" of Animals. Journal of Neuroscience 36(19):5373-5384.

Costantini M, Galati G, Ferretti A, Caulo M, Tartaro A, Romani GL, Aglioti SM. 2005. Neural systems underlying observation of humanly impossible movements: An fMRI study. Cerebral Cortex 15(11):1761-1767.

Craig AD. 2009. How do you feel--now? The anterior insula and human awareness. Nature reviews neuroscience 10(1).

Crittenden BM, Duncan J. 2014. Task Difficulty Manipulation Reveals Multiple Demand Activity but no Frontal Lobe Hierarchy. Cerebral Cortex 24(2):532-540.

Cukur T, Nishimoto S, Huth AG, Gallant JL. 2013. Attention during natural vision warps semantic representation across the human brain. Nature Neuroscience 16(6):763-+.

de Gelder B, de Borst AW, Watson R. 2015. The perception of emotion in body expressions. Wiley Interdisciplinary Reviews-Cognitive Science 6(2):149-158.

de Gelder B, Hortensius R, Tamietto M. 2012. Attention and awareness each influence amygdala activity for dynamic bodily expressions-a short review. Frontiers in Integrative Neuroscience 6.

de Gelder B, Poyo Solanas M. 2020. Body expression perception. A computational neuroethology perspective. Trends in Cognitive Sciences (Under review).

de Gelder B, Snyder J, Greve D, Gerard G, Hadjikhani N. 2004. Fear fosters flight: A mechanism for fear contagion when perceiving emotion expressed by a whole body. Proceedings of the National Academy of Sciences of the United States of America 101(47):16701-16706.

di Pellegrino G, Rafal R, Tipper SP. 2005. Implicitly evoked actions modulate visual selection: Evidence from parietal extinction. Current Biology 15(16):1469-1472.

Downing PE, Jiang YH, Shuman M, Kanwisher N. 2001. A cortical area selective for visual processing of the human body. Science 293(5539):2470-2473.

Downing PE, Peelen MV. 2011. The role of occipitotemporal body-selective regions in person perception. Cognitive Neuroscience 2(3-4):186-203.

Duncan J. 2001. An adaptive coding model of neural function in prefrontal cortex. Nature Reviews Neuroscience 2(11):820-829.

Duncan J. 2010. The multiple-demand (MD) system of the primate brain: mental programs for intelligent behaviour. Trends in Cognitive Sciences 14(4):172-179.

Engelen T, de Graaf TA, Sack AT, de Gelder B. 2015. A causal role for inferior parietal lobule in emotion body perception. Cortex 73:195-202.

Engelen T, Zhan M, Sack AT, de Gelder B. 2018. Dynamic Interactions between Emotion Perception and Action Preparation for Reacting to Social Threat: A Combined cTBS-fMRI Study. Eneuro 5(3).

Forman SD, Cohen JD, Fitzgerald M, Eddy WF, Mintun MA, Noll DC. 1995. Improved assessment of significant activation in fuctional magnetic-resonance-imagince (fMRI) - use of a cluster-size-threshold. Magnetic Resonance in Medicine 33(5):636-647.

Gardumi A, Ivanov D, Hausfeld L, Valente G, Formisano E, Uludag K. 2016. The effect of spatial resolution on decoding accuracy in fMRI multivariate pattern analysis. Neuroimage 132:32-42.

Goebel R, Esposito F, Formisano E. 2006. Analysis of Functional Image Analysis Contest (FIAC) data with BrainVoyager QX: From single-subject to cortically aligned group general linear model analysis and self-organizing group independent component analysis. Human Brain Mapping 27(5):392-401.

Goldberg H, Christensen A, Flash T, Giese MA, Malach R. 2015. Brain activity correlates with emotional perception induced by dynamic avatars. Neuroimage 122:306-317.

Goldberg H, Preminger S, Malach R. 2014. The emotion-action link? Naturalistic emotional stimuli preferentially activate the human dorsal visual stream. Neuroimage 84:254-264.

Goldman-Rakic PS. 1996. The prefrontal landscape: Implications of functional architecture for understanding human mentation and the central executive. Philosophical Transactions of the Royal Society of London Series B-Biological Sciences 351(1346):1445-1453.

Greve DN, Fischl B. 2009. Accurate and robust brain image alignment using boundary-based registration. Neuroimage 48(1):63-72.

Grezes J, Pichon S, de Gelder B. 2007. Perceiving fear in dynamic body expressions. Neuroimage 35(2):959-967.

Habel U, Windischberger C, Derntl B, Robinson S, Kryspin-Exner I, Gur RC, Moser E. 2007. Amygdala activation and facial expressions: Explicit emotion discrimination versus implicit emotion processing. Neuropsychologia 45(10):2369-2377.

Hajdúk M, Klein HS, Bass EL, Springfield CR, Pinkham AE. 2019. Implicit and explicit processing of bodily emotions in schizophrenia. Cognitive Neuropsychiatry:1-15.

Haxby JV, Connolly AC, Guntupalli JS. 2014. Decoding neural representational spaces using multivariate pattern analysis. Annu Rev Neurosci 37:435-56.

Hebart MN, Bankson BB, Harel A, Baker CI, Cichy RM. 2018. The representational dynamics of task and object processing in humans. Elife 7:21.

Hoshi E, Tanji J. 2007. Distinctions between dorsal and ventral premotor areas: anatomical connectivity and functional properties. Current Opinion in Neurobiology 17(2):234-242.

Huth AG, Nishimoto S, Vu AT, Gallant JL. 2012. A Continuous Semantic Space Describes the Representation of Thousands of Object and Action Categories across the Human Brain. Neuron 76(6):1210-1224.

Igelström KM, Graziano MSA. 2017. The inferior parietal lobule and temporoparietal junction: A network perspective. Neuropsychologia 105:70-83.

Jiang X, Bradley E, Rini RA, Zeffiro T, VanMeter J, Riesenhuber M. 2007. Categorization training results in shape- and category-selective human neural plasticity. Neuron 53(6):891-903.

Kana RK, Travers BG. 2012. Neural substrates of interpreting actions and emotions from body postures. Social Cognitive and Affective Neuroscience 7(4):446-456.

Kitada R, Johnsrude IS, Kochiyama T, Lederman SJ. 2010. Brain networks involved in haptic and visual identification of facial expressions of emotion: An fMRI study. Neuroimage 49(2):1677-1689.

Kriegeskorte N, Goebel R, Bandettini P. 2006. Information-based functional brain mapping. Proceedings of the National Academy of Sciences of the United States of America 103(10):3863-3868.

Kriegeskorte N, Mur M, Ruff DA, Kiani R, Bodurka J, Esteky H, Tanaka K, Bandettini PA. 2008. Matching categorical object representations in inferior temporal cortex of man and monkey. Neuron 60(6):1126-41.

Luckhardt C, Kröger A, Cholemkery H, Bender S, Freitag CM. 2017. Neural Correlates of Explicit Versus Implicit Facial Emotion Processing in ASD. Journal of Autism and Developmental Disorders 47(7):1944-1955.

Makris N, Kennedy DN, McInerney S, Sorensen AG, Wang R, Caviness VS, Pandya DN. 2005. Segmentation of subcomponents within the superior longitudinal fascicle in humans: A quantitative, in vivo, DT-MRI study. Cerebral Cortex 15(6):854-869.

Mars RB, Jbabdi S, Sallet J, O'Reilly JX, Croxson PL, Olivier E, Noonan MP, Bergmann C, Mitchell AS, Baxter MG et al. . 2011. Diffusion-Weighted Imaging Tractography-Based Parcellation of the Human Parietal Cortex and Comparison with Human and Macaque Resting-State Functional Connectivity. Journal of Neuroscience 31(11):4087-4100.

Marsh AA, Kozak MN, Wegner DM, Reid ME, Yu HH, Blair RJR. 2010. The neural substrates of action identification. Social Cognitive and Affective Neuroscience 5(4):392-403.

McKee JL, Riesenhuber M, Miller EK, Freedman DJ. 2014. Task Dependence of Visual and Category Representations in Prefrontal and Inferior Temporal Cortices. Journal of Neuroscience 34(48):16065-16075.

Mitchell TM, Shinkareva SV, Carlson A, Chang KM, Malave VL, Mason RA, Just MA. 2008. Predicting human brain activity associated with the meanings of nouns. Science 320(5880):1191-1195.

Moro V, Urgesi C, Pernigo S, Lanteri P, Pazzaglia M, Aglioti SM. 2008. The Neural Basis of Body Form and Body Action Agnosia. Neuron 60(2):235-246.

Nastase SA, Connolly AC, Oosterhof NN, Halchenko YO, Guntupalli JS, Castello MVD, Gors J, Gobbini MI, Haxby JV. 2017. Attention Selectively Reshapes the Geometry of Distributed Semantic Representation. Cerebral Cortex 27(8):4277-4291.

Ong W-Y, Stohler CS, Herr DR. 2019. Role of the Prefrontal Cortex in Pain Processing. Molecular Neurobiology 56(2):1137-1166.

Ongur D, Price JL. 2000. The organization of networks within the orbital and medial prefrontal cortex of rats, monkeys and humans. Cerebral Cortex 10(3):206-219.

Ontivero-Ortega M, Lage-Castellanos A, Valente G, Goebel R, Valdes-Sosa M. 2017. Fast Gaussian Naive Bayes for searchlight classification analysis. Neuroimage 163:471-479.

Oosterhof NN, Wiggett AJ, Diedrichsen J, Tipper SP, Downing PE. 2010. Surface-Based Information Mapping Reveals Crossmodal Vision-Action Representations in Human Parietal and Occipitotemporal Cortex. Journal of Neurophysiology 104(2):1077-1089.

Orgs G, Dovern A, Hagura N, Haggard P, Fink GR, Weiss PH. 2015. Constructing Visual Perception of Body Movement with the Motor Cortex. Cerebral Cortex 26(1):440-449.

Peelen MV, Atkinson AP, Andersson F, Vuilleumier P. 2007. Emotional modulation of body-selective visual areas. Social Cognitive and Affective Neuroscience 2(4):274-283.

Peelen MV, Atkinson AP, Vuilleumier P. 2010. Supramodal Representations of Perceived Emotions in the Human Brain. Journal of Neuroscience 30(30):10127-10134.

Peelen MV, Downing PE. 2007. The neural basis of visual body perception. Nature Reviews Neuroscience 8(8):636-648.

Peelen MV, Downing PE. 2017. Category selectivity in human visual cortex: Beyond visual object recognition. Neuropsychologia 105:177-183.

Peelen MV, Fei-Fei L, Kastner S. 2009. Neural mechanisms of rapid natural scene categorization in human visual cortex. Nature 460(7251):94-U105.

Pichon S, de Gelder B, Grezes J. 2009. Two different faces of threat. Comparing the neural systems for recognizing fear and anger in dynamic body expressions. Neuroimage 47(4):1873-1883.

Pichon S, de Gelder B, Grezes J. 2012. Threat Prompts Defensive Brain Responses Independently of Attentional Control. Cerebral Cortex 22(2):274-285.

Poyo Solanas M, Vaessen M, de Gelder B. 2020. Limb contraction drives fear perception. bioRxiv:2020.01.09.899849.

Poyo Solanas M, Zhan MY, Vaessen M, Hortensius R, Engelen T, de Gelder B. 2018. Looking at the face and seeing the whole body. Neural basis of combined face and body expressions. Social Cognitive and Affective Neuroscience 13(1):135-144.

Ross P, Atkinson AP. 2020. Expanding Simulation Models of Emotional Understanding: The Case for Different Modalities, Body-State Simulation Prominence, and Developmental Trajectories. Frontiers in Psychology 11:21.

Ross P, de Gelder B, Crabbe F, Grosbras MH. 2019. Emotion modulation of the body-selective areas in the developing brain. Developmental Cognitive Neuroscience 38.

Salomon R, Ronchi R, Dönz J, Bello-Ruiz J, Herbelin B, Martet R, Faivre N, Schaller K, Blanke O. 2016. The Insula Mediates Access to Awareness of Visual Stimuli Presented Synchronously to the Heartbeat. The Journal of neuroscience : the official journal of the Society for Neuroscience 36(18):5115-5127.

Sarkheil P, Goebel R, Schneider F, Mathiak K. 2013. Emotion unfolded by motion: a role for parietal lobe in decoding dynamic facial expressions. Social Cognitive and Affective Neuroscience 8(8):950-957.

Saxe R, Jamal N, Powell L. 2006. My body or yours? The effect of visual perspective on cortical body representations. Cerebral Cortex 16(2):178-182.

Sha L, Haxby JV, Abdi H, Guntupalli JS, Oosterhof NN, Halchenko YO, Connolly AC. 2015. The Animacy Continuum in the Human Ventral Vision Pathway. Journal of Cognitive Neuroscience 27(4):665-678.

Sinke CBA, Van den Stock J, Goebel R, de Gelder B. 2012. The Constructive Nature of Affective Vision: Seeing Fearful Scenes Activates Extrastriate Body Area. Plos One 7(6).

Stienen BMC, Tanaka A, de Gelder B. 2011. Emotional Voice and Emotional Body Postures Influence Each Other Independently of Visual Awareness. Plos One 6(10).

Tamietto M, Cauda F, Celeghin A, Diano M, Costa T, Cossa FM, Sacco K, Duca S, Geminiani GC, de Gelder B. 2015. Once you feel it, you see it: Insula and sensory-motor contribution to visual awareness for fearful bodies in parietal neglect. Cortex 62:56-72.

Tsotsos JK. 2011. A computational perspective on visual attention. MIT Press.

Van den Stock J, de Jong SJ, Hodiamont PPG, de Gelder B. 2011. Perceiving emotions from bodily expressions and multisensory integration of emotion cues in schizophrenia. Social Neuroscience 6(5-6):537-547.

Van den Stock J, Hortensius R, Sinke C, Goebel R, de Gelder B. 2015. Personality traits predict brain activation and connectivity when witnessing a violent conflict. Scientific Reports 5.

Vangeneugden J, Peelen MV, Tadin D, Battelli L. 2014. Distinct Neural Mechanisms for Body Form and Body Motion Discriminations. The Journal of Neuroscience 34(2):574-585.

Vuilleumier P, George N, Lister V, Armony J, Driver J. 2005. Effects of perceived mutual gaze and gender on face processing and recognition memory. Visual Cognition 12(1):85-101.

Vuilleumier P, Richardson MP, Armony JL, Driver J, Dolan RJ. 2004. Distant influences of amygdala lesion on visual cortical activation during emotional face processing. Nature Neuroscience 7(11):1271-1278.

Wager T. 2008. The roles of medial prefrontal cortex in emotion: Neuroimaging evidence for functional subdivisions and cortical-subcortical pathways. Biological Psychiatry 63(7):151S-151S.

Watson R, de Gelder B. 2017. How white and black bodies are perceived depends on what emotion is expressed. Scientific Reports 7.

Weiner KS, Grill-Spector K. 2011. Not one extrastriate body area: Using anatomical landmarks, hMT+, and visual field maps to parcellate limb-selective activations in human lateral occipitotemporal cortex. Neuroimage 56(4):2183-2199.

Weiner KS, Grill-Spector K. 2012. The improbable simplicity of the fusiform face area. Trends in Cognitive Sciences 16(5):251-254.

Xu YD, Vaziri-Pashkam M. 2019. Task modulation of the 2-pathway characterization of occipitotemporal and posterior parietal visual object representations. Neuropsychologia 132.

Zhan MY, Goebel R, de Gelder B. 2018. Ventral and Dorsal Pathways Relate Differently to Visual Awareness of Body Postures under Continuous Flash Suppression. Eneuro 5(1).

Zimmermann M, Mars RB, de Lange FP, Toni I, Verhagen L. 2018. Is the extrastriate body area part of the dorsal visuomotor stream? Brain Structure and Function 223(1):31-46.

Zimmermann M, Verhagen L, de Lange FP, Toni I. 2016. The Extrastriate Body Area Computes Desired Goal States during Action Planning. eNeuro 3(2):ENEURO.0020-16.2016.